Interfacial Molecular Searching Using Forager Dynamics

Jon H. Monserud and Daniel K. Schwartz

Phys. Rev. Lett. **116**, 098303 — Published 4 March 2016

DOI: 10.1103/PhysRevLett.116.098303

Interfacial Molecular Searching Using Forager Dynamics

Jon H. Monserud and Daniel K. Schwartz*

Department of Chemical and Biological Engineering

University of Colorado Boulder, Boulder, Colorado 80309

*To whom correspondence should be addressed: daniel.schwartz@colorado.edu

Summary

Many biological and technological systems employ efficient non-Brownian intermittent search strategies where localized searches alternate with long flights. Coincidentally, molecular species exhibit intermittent behavior at the solid/liquid interface, where periods of slow motion are punctuated by fast flights through the liquid phase. Single-molecule tracking was used here to observe the interfacial search process of DNA for complementary DNA. Measured search times were qualitatively consistent with an intermittent-flight model, and ~10-times faster than equivalent Brownian searches, suggesting that molecular searches for reactive sites benefit from similar efficiencies as biological organisms.

Search processes play important roles in ecological [1-3], military [4, 5], and molecular systems that comprise applications in (bio)chemical reactions [6, 7], chemical sensing / bioassays [8, 9], signal transduction in biomembranes [10, 11], and others [12, 13]. In these systems, a similar challenge is encountered: What strategy should searchers employ to find target sites efficiently? Effective searches comprise several components, including the searcher's knowledge, range of detection, search rate, target density, and search strategy [14]. While some organisms employ knowledge or active detection as part of searching (*e.g.* chemotaxis), "foraging" refers to the stochastic knowledge-free phase of searching. A foraging search is considered complete when the searcher comes within the detection range of its target [5], *e.g.* when predator visually detects prey. In molecular systems, a search is entirely knowledge-free and the detection range is defined by the *reaction radius* (*a*). The characteristic rate of the search is determined by the speed with which the predator hunts its prey or the diffusion coefficient (*D*) of a molecular search, and the search is universally minimized for the greatest search rate that is accessible to the searcher [15]. The efficiency of a given search strategy may depend on the target density, which is statistically related to the average starting distance between searcher and target (*R*) [16].

Search strategies cover a wide range of possibilities [17]. For example, bears hunting salmon during the spawning run know where to find the salmon, and the static search is mostly a question of waiting for a salmon to appear [14]. Another strategy, involving 1D diffusion along a chain alternating with jumps across loops in the chain, is observed in protein-DNA interactions [18, 19]. Yet other strategies involve alternating diffusion and static capture [20], bearing a superficial resemblance to observations of interfacial molecular diffusion, which alternates between periods of "flying" and "crawling" at the solid-liquid interface [21].

It has been hypothesized that in a system where targets are sparse, searchers should adopt an *intermittent search* strategy of short-range searches with occasional longer (non-searching) flights [22-24]. A particular realization of this involves a so-called continuous time random walk (CTRW) process where the non-searching flight-lengths are drawn from a Pareto-Lévy distribution [25-27]. When targets are abundant, Brownian motion is a sufficiently effective strategy [1]. However, in ecological, physical, and chemical systems, theory predicts that intermittent searches are often more efficient than pure Brownian behavior for locating randomly distributed targets [14, 28].

Interestingly, recent observations by our group and others suggest that the behavior of surface-adsorbed molecules qualitatively mimics the motion favored for sparse prey searches [29-32]. In particular, proteins, polymers and small molecules all exhibit intermittent motion that corresponds to a CTRW with periods of slow or confined local diffusion alternating with flights comprising a heavy-tailed distribution. These observations are consistent with longstanding theoretical models [33-37] that predict similar phenomena due to "desorption-mediated diffusion", *i.e.* the notion that interfacial motion of adsorbed molecules includes a series of three-dimensional hops (which can be long) through an adjacent liquid phase. This coincidental similarity between molecular transport at interfaces and biologically-evolved forager dynamics suggests molecular searching may be enhanced under sparse target conditions.

To directly test theoretical models used to describe forager dynamics [1, 15, 38-40], we developed a system permitting the direct observation of two-dimensional (2D) interfacial molecular searching. Specifically, we performed high-throughput (>600,000 individual trajectories) dynamic single molecule (SM) studies of hybridization between mobile and tethered DNA at solid-liquid interfaces. Total internal reflection fluorescence microscopy (TIRFM) [41] was used in conjunction with intermolecular Förster

resonance energy transfer (FRET) and alternating laser excitation, allowing direct quantitative analysis of molecular search behavior as a function of initial searcher-target distance [42, 43] These search times were directly compared to theoretical predictions based on Brownian searching and intermittent desorption-mediated searching respectively [15].

Fused silica wafers were initially modified with epoxide-silane chemistry, and subsequently modified with either zinc-thiolate-disulfide[44] or lithium hydroxide catalyzed thiol-epoxide chemistry[45] to covalently attach DNA to the surface along with either a "hydrophobic" (2-(pentyldisulfanyl)pentane) or "hydrophilic" (methyl-PEG4-thiol) moiety. Sessile drop contact angle experiments were used to assess hydrophobicity [46], and yielded values of 70° ± 2° and 20° ± 3° for hydrophobic and hydrophilic surfaces respectively. Surfaces for negative control experiments were prepared by performing surface modifications in the absence of DNA.

Intermolecular FRET from donor (AlexaFluor® 488) to acceptor (Quasar®-670) fluorophores [47], was used to identify the timing and location of successful searches. In our experiments, acceptor-labeled ssDNA was immobilized to a surface that was exposed to aqueous solutions (1x PBS, pH = 7.4) of the donor-labeled complementary strand (or a non-complementary control strand). More detailed discussion of the experimental design is described in the Supplementary Material [48-53]. Dual-channel image sequences of all surfaces were acquired, comprising >600,000 molecular trajectories for the complementary strands; molecules that resided on the surface for $\leq$100ms (1 frame) were excluded from further analysis. Emission intensities of molecules were monitored in donor and acceptor channels, and observation of acceptor emission above a selected threshold was used to identify a successful search event (Figure S1). A discussion of the "hybridization" threshold is included in the Supplementary Materials [48].

In these TIRFM experiments, only donor-labeled DNA molecules that had adsorbed to the interface were resolved (Figure 1A, first frame); un-adsorbed molecules near the surface were blurred because of their rapid motion and contributed only to background fluorescence. Adsorbed molecules were observed to move stochastically within the field of view, exhibiting apparent intermittent motion involving alternating slow/confined walks and long flights (Figure 1A, second frame). Some molecules (~20-40% of trajectories) eventually located an immobilized complementary strand and hybridized, causing acceptor emission *via* FRET (Figure 1A, third frame). Immobilized DNA locations were identified by periodic direct excitation of acceptor fluorophores, permitting the calculation of the initial "starting-distance" between each adsorbing donor-labeled DNA molecule and the nearest immobilized complementary strand (see details in the Supplementary Materials [48]).

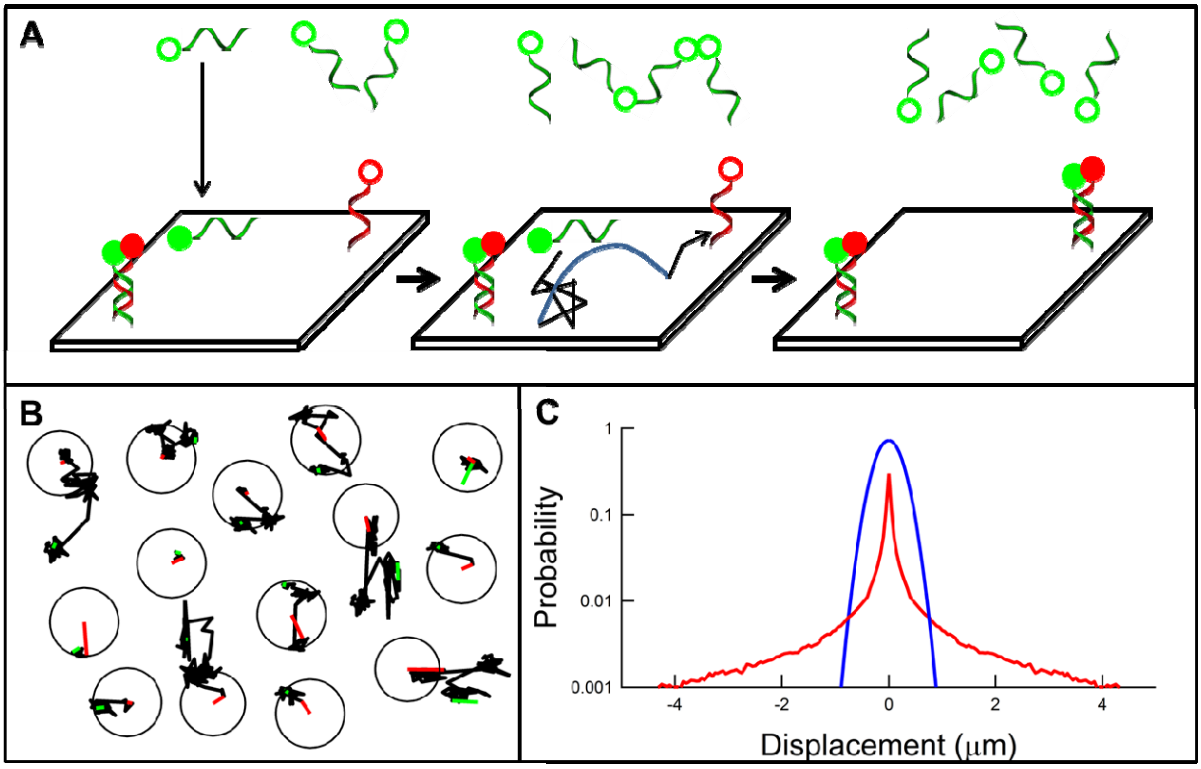

Figure 1. (A) physical interpretation of observations. In all parts of the figure, donor fluorophores are represented in green and acceptor fluorophores in red. (B) Example trajectories of successful Molecular searches. A circle indicates a starting distance of 0.5μm. First step of the trajectories (-) and the last step of the trajectories (-). (C) Step size distribution of DNA Molecules on a hydrophobic Surface (--). Gaussian distribution using the mean diffusion coefficient of DNA molecules on a hydrophobic Surface (--). The integrals of these distributions were normalized to unity.

The representative trajectories plotted in Figure 1B demonstrate intermittent non-Brownian behavior of a molecular search where molecules alternate between large displacements and slow confined walks. To quantify this behavior, the normalized distribution of all DNA displacements on hydrophobic surfaces (red) was compared to a Gaussian distribution (blue) representing the same mean diffusion coefficient (Figure 1C). The integrals of the distributions were normalized to unity. These data represent the probability that a molecule has moved a given displacement along the x or y coordinate during time Δt. Consistent with previous observations for a variety of molecules at the solid-liquid interface [29, 32], the

experimental distribution is clearly non-Gaussian, but comprises a narrow Gaussian peak and extended tails. In contrast with the Gaussian distribution (blue line in Figure 1C), where steps longer than ~1 μm have negligible probability, the experimental distribution (red line) exhibits heavy non-Gaussian tails that extend to flights as long as 4μm.

Notably, as shown in figure 1B, where the final trajectory steps are colored red, hybridization occurred at various stages of the intermittent motion, *i.e.* not only following a flight, but also after various periods of local searching. These combined observations suggested the molecular searching of DNA was non-Brownian and qualitatively similar to the type of intermittent search strategy described above.

The observation of molecular association events on the basis of FRET efficiency was used to calculate the distribution of first passage times (the time interval between initial adsorption and successful hybridization) and the search success as a function of the initial searcher-target, *R*. The fraction of

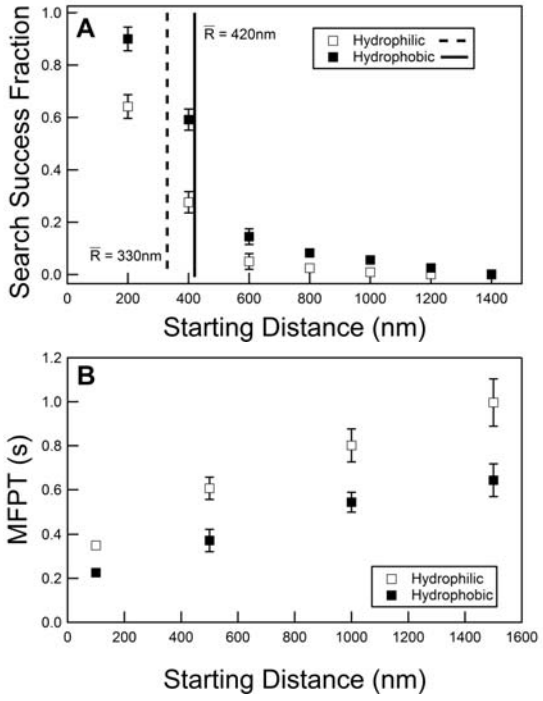

Figure 2. (A) Search efficiency of molecules as a function of initial distance-to-target for hydrophobic (□) and hydrophilic (■) surfaces. The vertical lines indicate the mean search radius, $\bar{R}$ for hydrophobic (-) and hydrophilic (- -) surfaces. (B) Mean first passage times for molecules as a function of initial distance-to-target for hydrophobic (□) and hydrophilic (■) surfaces

successful searches was calculated for trajectories beginning at various starting distances (±50 nm) from these target sites (Figure 2A). For example, trajectories beginning within an annulus spanning 950–1050 nm in radius were included in the analysis for the *R*=1000 nm. Unsurprisingly, both surfaces approached a search success fraction of unity *for R* = 0 nm and the successful fraction decreased systematically with increasing *R*, with success becoming rare for *R* > 1200 nm. Notably, the search success fraction declined more rapidly with distance on the hydrophilic surface compared with the hydrophobic interface. For example, for *R*=400 nm, ~60% of searches were successful on hydrophobic surfaces, but only ~25% on hydrophilic surfaces. In previous work, we found that ssDNA surface dynamics were strongly influenced by the physicochemical properties of a surface, including hydrophobicity [54]. These observations demonstrated that for short DNA lengths (<25 bases) diffusion was enhanced and surface residence times reduced on more hydrophobic surfaces. Similar observations were made here, as shown in Supplemental Material Figures S2 and S3 [48]. Therefore, we hypothesized that the difference in search efficiency on hydrophobic and hydrophilic surfaces was related to the characteristic size of the region explored by a DNA molecule prior to desorption. To estimate this mean search radius, $\overline{\boldsymbol{R}}$, the radius of gyration was calculated for each trajectory, the cumulative search radius distributions were accumulated, fit with an exponential-mixture model, and used to calculate the mean search radius, $\overline{\boldsymbol{R}}$. (See Supplemental Material for more details, including Figure S4 [48]). The mean search radii calculated were 330 ± 50nm and 420 ± 60nm for hydrophilic and hydrophobic surfaces respectively, shown as vertical lines in Figure 2A, which suggests a strong correlation between the mean search radius and the successful fraction. In particular, for each surface chemistry type, the mean search radius represents the approximate distance at which 50% of searches were successful.

Using only trajectories associated with successful searches, the first passage times were calculated for trajectories with various *R* values. The mean first passage times (MFPT) are shown in Figure 2B, and the

first passage time distributions are included in Supplemental Material Figure S5 [48]. The MFPTs were systematically smaller (by nearly a factor of two) on hydrophobic surfaces than on hydrophilic surfaces, consistent with the faster diffusion on hydrophobic surfaces as described previously. Moreover, as expected, the MFPTs increased systematically with increasing *R* from 100–1500 nm, ranging from ~0.4–1 s on hydrophilic surfaces and 0.2–0.6 s on hydrophobic surfaces.

As mentioned above, under sparse target conditions (as in these experiments) intermittent search strategies are predicted to exhibit improved efficiency. To determine if interfacial molecular searches benefit from these dynamics, we compared the experimental results with two theoretical models, both developed by Benichou and co-workers, which predict the mean first passage time (*i.e.* the average search time) using different physical assumptions.

The first model (BM) describes continuous Brownian motion, where a searcher performs regular short displacements while searching for a target. The MFPT for this model [40], $\langle T_{BM} \rangle$, is given by

$$\langle T_{BM} \rangle = \frac{A}{2\pi \bar{D}} \ln \frac{R}{a} \qquad (1)$$

where $\bar{D}$ is the mean diffusion coefficient, *R* is the initial distance between searcher and target, *a* is the reaction radius (*i.e.* the detection range), and *A* is the search domain area. The reaction radius, *a*, was taken to be the radius of gyration of the probe molecule, 0.54 nm. In Equation 1, *A* was estimated using the approximate average distance between target molecules, i.e. $A = \pi(2\ \mu m)^2$.

The second intermittent flight model (IF), associated with intermittent interfacial searching involving long-flights, describes short rapid interfacial searches alternating with desorption-mediated flights; the MFPT of this model [15], $\langle \overline{T_{IF}} \rangle$, averaged over all starting distances within the search domain, is given by

$$\langle\overline{T_{IF}}\rangle = \overline{\tau_w}\frac{\left[\left(\frac{\sqrt{A}}{a\pi}\right)^2 - 1\right]\overline{X_v} + \frac{2}{a}\sqrt{D_2\overline{\tau_w}}\,\overline{Y_v}}{\overline{X_v} - \frac{2}{a}\sqrt{D_2\overline{\tau_w}}\,\overline{Y_v}} \qquad (2)$$

where X_v and Y_v are functions containing the modified Bessel functions $I_v(a, D_2, A, \overline{\tau_w})$ and $K_v(a, D_2, A, \overline{\tau_w})$ as described in the Supplementary Material [48]. A and a are the search domain size and reaction radius respectively, D_2 is the diffusion coefficient associated with the slow searching time intervals, and $\overline{\tau_w}$ is the mean waiting time between desorption-mediated flights.

Unlike Equation 1, which incorporates an explicit starting distance R, $\langle\overline{T_{IF}}\rangle$ given by Equation 2 represents the integrated MFPT for all molecules that start, with equal spatial probability, within a confined circular search domain of area $A=\pi r^2$(where r is the domain radius), and search until they find the target. To estimate MFPT values for comparison with the experimentally measured data, we noted that the measured quantity (the MFPT for molecules starting within a narrow annulus centered at a distance R) could be approximately related to the incremental change of the integrated MFPT $\langle\overline{T_{IF}}\rangle$ upon the addition of an infinitesmal outer annulus, i.e. the derivative of $\langle\overline{T_{IF}}\rangle$ with respect to r. Therefore, accounting for geometric factors associated with differentiation in polar coordinates, we compared the data to calculated values using the expression $MFPT = \frac{r}{2}\frac{d\langle\overline{T_{IF}}\rangle}{dr}$, evaluated at $r=R$. For this calculation, Equation 2 was differentiated numerically using the explicit Runge Kutta method (NDSolve, Mathematica®). We emphasize that this calculation represented only an approximate way to estimate theoretical MFPT values for comparison with the experimental data, since it was not possible to completely disentangle effects related to starting distance and domain size in this way. Moreover, we note that the IF model incorporates assumptions not perfectly matched to the experimental system. Most importantly, the DNA molecules were not confined, and could desorb prior to finding their targets, resulting in a measured distribution of successful search times that was skewed to smaller values than predicted by the full ensemble considered in the model, where searchers continued until successful.

All parameters (D, D_2,$\overline{\tau_w}$) were determined from control experiments in the absence of target DNA, and used to calculate solutions to each model without adjustment. To calculate $\overline{\tau_w}$, we measured waiting times by defining a distance threshold of 0.15 μm to distinguish large displacements from smaller diffusive steps. A cumulative probability distribution of these waiting time intervals is shown in Supplemental Material Figure S6 [48]. The distributions of waiting times were fit with an exponential mixture model; characteristic waiting times and their respective population fractions were extracted from these fits and used to calculate $\overline{\tau_w}$=0.307 ± 0.001 s and $\overline{\tau_w}$=0.192 ± 0.003 s for the hydrophilic and hydrophobic surfaces, respectively.. To calculate $\overline{D}$, the squared-displacement was calculated for each step of each trajectory. Experimental cumulative squared-displacement distributions were created by sorting the squared-displacement data and ranking each data point [55]. The cumulative squared-displacement distributions (Supplemental Material Figure S3 [48]) were fit with a Gaussian-mixture model. Characteristic diffusion coefficients and their respective population fractions were extracted from these fits and were used to calculate $\overline{D}$=0.209 ± 0.001 μm^2/s for the hydrophilic surface and $\overline{D}$=0.375 ± 0.001 μm^2/s for the hydrophobic surface. As described in previous work, the surface diffusion coefficient associated with the slow searching intervals, D_2, was identified as the crawling or slow diffusion mode and extracted from cumulative squared-displacement distributions [56, 57], giving values of D_2=0.044 ± 0.001 μm^2/s and D_2=0.058 ± 0.001 μm^2/s for the hydrophilic and hydrophobic surfaces, respectively.

The results of these calculations are shown along with the experimental MFPT values in Figure 3 for both hydrophobic and hydrophilic surfaces. We emphasize that these theoretical predictions used experimentally-measured values as inputs, with minimal assumptions, and no adjustable parameters. A sensitivity analysis was performed on the IF-model to determine the parameter with the largest impact on the predicted values, and it was found to be most sensitive to changes in diffusion coefficient D_2. Therefore, the IF-model was calculated while varying the diffusion coefficients by a factor of 2, and the results of these calculations are shown as the shaded regions in Figure 3.

The rapid decrease in MFPT predicted by the IF model for small values of R is clearly not reflected in the experimental measurements. This is an artifact of the experimental temporal resolution, which involves sequences of images captured at intervals of 0.1 s. Due to this non-zero acquisition time, the minimum

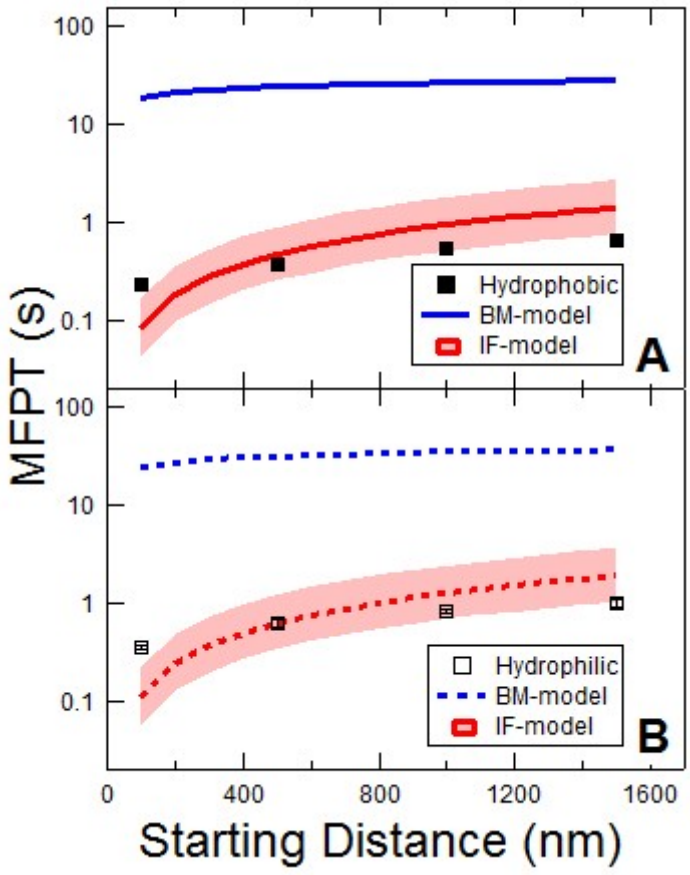

Figure 3. Semi-logarithmic plots of mean first passage times for molecules starting searches from a starting distance from target for (A) hydrophobic (□) and (B) hydrophilic surfaces (□), including the results of Brownian motion (--) and Intermittent flight (--) models.

measurable time for a trajectory is 0.2 s, and the measured MFPT is therefore noticeably biased towards larger values in the near-target regime.

Importantly, for both surface chemistries the MFPTs given by the BM-model exceed the experimental results by at least one order of magnitude. Thus, molecules identify their targets more than ten times faster than expected for molecules executing a simple random walk with the same apparent mean diffusion coefficient. This dramatic effect is due to the highly non-Gaussian nature of the step-size distributions shown in Figure 1C and Supplemental Material Figure S3 [48]. It is remarkable that this enhanced search process happens to duplicate similar strategies that have evolved throughout the biological world. Significantly, the IF-model captures the correct order of magnitude of measured MFPT data for both hydrophobic and hydrophilic surfaces with no adjustable parameters. In particular, the agreement is within a factor of two or less for all observed points except in the near-target regime. This is noteworthy, considering the various simplifying assumptions incorporated into the theory.

In addition to revealing the different mechanisms associated with surface searching, a detailed analysis of molecular trajectories also provided kinetic information about the dynamics of DNA denaturing/melting. Each hybridization event was dynamic, and ultimately ended *via* a transition back to a searching state or desorption, the mechanisms of which were described previously [42]. Comparison of the two surfaces demonstrates that the duplex DNA was longer lived on the hydrophilic surface with a mean characteristic melting time of ~1.9 s, compared to the hydrophobic surface where the mean characteristic melting time was ~1.3 s. These observations, combined with the analysis of searching, suggest that for these DNA sequences, the hydrophobic surface resulted in faster, more efficient DNA searching but reduced the longevity of duplex DNA. The raw data and a more detailed discussion of the DNA melting kinetics are included in the Supplemental Material (Figure S7) [48].

The authors gratefully acknowledge support from the National Institute of Biomedical Imaging and Bioengineering of the NIH (5R21EB015061-02). Additional support was provided by the NSF (award #CHE-1306108) for DKS and for the development of single-molecule FRET tracking methods.

References

[1] G. M. Viswanathan, S. V. Buldyrev, S. Havlin, M. G. E. da Luz, E. P. Raposo, and H. E. Stanley, Nature **401**, 911 (1999).
[2] A. M. Edwards *et al.*, Nature **449**, 1044 (2007).
[3] S. Condamin, O. Benichou, and J. Klafter, Phys Rev Lett **98** (2007).
[4] M. F. Shlesinger, Nature **443**, 281 (2006).
[5] J. R. Newman, *The world of mathematics; a small library of the literature of mathematics from Ah-mosé the scribe to Albert Einstein* (Simon and Schuster, New York,, 1956), Vol. 4, p.^pp. 2160-2181.
[6] M. Coppey, O. Bénichou, R. Voituriez, and M. Moreau, Biophysical Journal **87**, 1640.
[7] O. G. Berg and C. Blomberg, Biophysical Chemistry **4**, 367 (1976).
[8] M. Schena, D. Shalon, R. W. Davis, and P. O. Brown, Science **270**, 467 (1995).
[9] L. P. Lim, N. C. Lau, P. Garrett-Engele, A. Grimson, J. M. Schelter, J. Castle, D. P. Bartel, P. S. Linsley, and J. M. Johnson, Nature **433**, 769 (2005).
[10] M. Falk, M. Klann, M. Reuss, and T. Ertl, in *2010 IEEE International Symposium on Biomedical Imaging: From Nano to Macro* (2010), pp. 1301.
[11] M. P. Clausen and B. C. Lagerholm, Nano Letters **13**, 2332 (2013).
[12] S. A. Rice, *Diffusion-limited reactions* (Elsevier, Amsterdam ; New York, 1985), Comprehensive chemical kinetics, 25.
[13] P. Hanggi, P. Talkner, and M. Borkovec, Rev Mod Phys **62**, 251 (1990).
[14] M. F. Shlesinger, J Phys a-Math Theor **42** (2009).
[15] O. Benichou, C. Loverdo, M. Moreau, and R. Voituriez, Physical chemistry chemical physics : PCCP **10**, 7059 (2008).
[16] G. M. Viswanathan, *The physics of foraging : an introduction to random searches and biological encounters* (Cambridge University Press, Cambridge ; New York, 2011).
[17] F. S. Michael, Journal of Physics A: Mathematical and Theoretical **42**, 434001 (2009).
[18] I. Eliazar, T. Koren, and J. Klafter, The Journal of Physical Chemistry B **112**, 5905 (2008).
[19] M. A. Lomholt, T. Ambjörnsson, and R. Metzler, Physical Review Letters **95**, 260603 (2005).
[20] O. Bénichou, C. Loverdo, M. Moreau, and R. Voituriez, Physical Review E **74**, 020102 (2006).
[21] N. Nelson, R. Walder, and D. K. Schwartz, Langmuir **28**, 12108 (2012).
[22] S. Ornes, Proceedings of the National Academy of Sciences **110**, 3202 (2013).
[23] F. BARTUMEUS, Fractals **15**, 151 (2007).
[24] G. M. Viswanathan, E. P. Raposo, and M. G. E. da Luz, Physics of Life Reviews **5**, 133 (2008).
[25] H. E. Stanley and N. Ostrowsky, *On growth and form : fractal and non-fractal patterns in physics* (M. Nijhoff, Dordrecht Netherlands ; Boston, 1986), NATO ASI series Series E, Applied sciences, no 100.
[26] S. Foss, T. Konstantopoulos, and S. Zachary, J Theor Probab **20**, 581 (2007).
[27] N. E. Humphries *et al.*, Nature **465**, 1066 (2010).
[28] P. Buividovich and Y. Makeenko, Nucl Phys B **834**, 453 (2010).
[29] M. Skaug, J. Mabry, and D. Schwartz, Physical Review Letters **110**, 256101 (2013).
[30] M. J. Skaug, J. N. Mabry, and D. K. Schwartz, Journal of the American Chemical Society **136**, 1327 (2013).
[31] S. C. Bae and S. Granick, Annual Review of Physical Chemistry **58**, 353 (2007).
[32] C. Yu, J. Guan, K. Chen, S. C. Bae, and S. Granick, Acs Nano **7**, 9735 (2013).
[33] O. Bychuk and B. O'Shaughnessy, Physical Review Letters **74**, 1795 (1995).
[34] O. V. Bychuk and B. O'Shaughnessy, The Journal of Chemical Physics **101**, 772 (1994).
[35] S. Stapf, R. Kimmich, and R. O. Seitter, Physical Review Letters **75**, 2855 (1995).
[36] R. Metzler and J. Klafter, Physics Reports **339**, 1 (2000).

[37] R. Metzler, W. G. Glöckle, and T. F. Nonnenmacher, Physica A: Statistical Mechanics and its Applications **211**, 13 (1994).
[38] R. D. Astumian and P. B. Chock, The Journal of Physical Chemistry **89**, 3477 (1985).
[39] S. Condamin, O. Benichou, V. Tejedor, R. Voituriez, and J. Klafter, Nature **450**, 77 (2007).
[40] S. Condamin, O. Bénichou, and M. Moreau, Phys Rev Lett **95**, 260601 (2005).
[41] A. Honciuc, A. W. Harant, and D. K. Schwartz, Langmuir **24**, 6562 (2008).
[42] J. H. Monserud and D. K. Schwartz, Acs Nano **8**, 4488 (2014).
[43] M. Kastantin and D. K. Schwartz, Acs Nano **5**, 9861 (2011).
[44] B. Movassagh, S. Sobhani, F. Kheirdoush, and Z. Fadaei, Synthetic Communications **33**, 3103 (2003).
[45] S. De and A. Khan, Chemical Communications **48**, 3130 (2012).
[46] F. M. Fowkes, W. A. Zisman, and American Chemical Society. Division of Colloid and Surface Chemistry., *Contact angle, wettability and adhesion; the Kendall award symposium honoring William A. Zisman, Los Angeles, Calif., April 2-3, 1963* (American Chemical Society, Washington,, 1964), Advances in chemistry series,, 43.
[47] J. R. Lakowicz, *Principles of fluorescence spectroscopy* (Springer, New York, 2006), 3rd edn.
[48] See Supplemental Material at [url] for supplementary discussion and figures, which includes Refs [49-53].
[49] D. J. Igor Luzinov, Andrea Liebmann-Vinson, Tricia Cregger, Mark D. Foster, and Vladimir V. Tsukruk, Langmuir **16**, 504 (2000).
[50] T. S. Work and E. Work, *Laboratory techniques in biochemistry and molecular biology* (North-Holland Pub. Co., Amsterdam,, 1969).
[51] H. Sahoo, Journal of Photochemistry and Photobiology C: Photochemistry Reviews **12**, 20 (2011).
[52] R. Walder and D. K. Schwartz, Langmuir **26**, 13364 (2010).
[53] M. Kastantin, B. B. Langdon, E. L. Chang, and D. K. Schwartz, Journal of the American Chemical Society **133**, 4975 (2011).
[54] J. H. Monserud and D. K. Schwartz, Biomacromolecules **13**, 4002 (2012).
[55] A. Honciuc, A. W. Harant, and D. K. Schwartz, Langmuir **24**, 6562 (2008).
[56] R. Walder, N. Nelson, and D. K. Schwartz, Physical Review Letters **107**, 156102 (2011).
[57] A. Honciuc and D. K. Schwartz, Journal of the American Chemical Society **131**, 5973 (2009).